Internal and External Catalysis in Boronic Ester Networks

Boyeong Kang and Julia A. Kalow*

Department of Chemistry, Northwestern University, 2145 Sheridan Rd., Evanston, IL 60208, USA
*E-mail: jkalow@northwestern.edu

Abstract: In dynamic materials, the reversible condensation between boronic acids and diols provides adaptability, self-healing ability, and responsiveness to small molecules and pH. The thermodynamics and kinetics of bond exchange determine the mechanical properties of dynamic polymer networks. Here, we investigate the effects of diol structure and salt additives on the rate of boronic acid–diol bond exchange, binding affinity, and the mechanical properties of the corresponding polymer networks. We find that proximal amides used to conjugate diols to polymers and buffering anions induce significant rate acceleration consistent with internal and external catalysis, respectively. This rate acceleration is reflected in the stress relaxation of the gels. These findings contribute to the fundamental understanding of the boronic ester dynamic bond and offer molecular strategies to tune the macromolecular properties of dynamic materials.

The reversible condensation between boronic acids and diols has been applied to sensors,[1-6] drug delivery,[3, 6-9] and dynamic hydrogels[3, 6, 8, 10] due to its biocompatibility, selectivity, and reactivity under ambient-temperature aqueous conditions. Among dynamic covalent chemistries[11-13], boronic acid–diol exchange offers the fastest uncatalyzed rates, enabling rapid responses to physical and chemical stimuli.[1, 14, 15] Within polymer networks, boronic esters endow self-healing behavior, stimuli responsiveness, and viscoelasticity. Experiment, simulations, and theory have revealed that the macroscopic properties of dynamic networks are highly dependent on the thermodynamics and kinetics of the reversible crosslink.[16-27] Specifically, the equilibrium constant (K_{eq}) of the dynamic reaction determines crosslink density in networks, and thus the stiffness of the polymer network (frequency-independent plateau modulus, G_{p}) (**Figure 1a**). On the other hand, important dynamic behaviors such as self-healing and viscoelasticity are governed by the kinetics of the reversible reaction. In dynamic networks that undergo exchange through dissociative mechanisms, the rate of dissociation (k_{r}) is thought to determine the viscoelasticity of the network, which is characterized by the crossover frequency (ω_{c}) at which material transition occurs from solid-like to liquid-like behavior (**Figure 1a**). Therefore, to better control and design boronic ester-based materials for specific applications, it is essential to understand the molecular factors that influence both kinetics and thermodynamics of this dynamic bond.

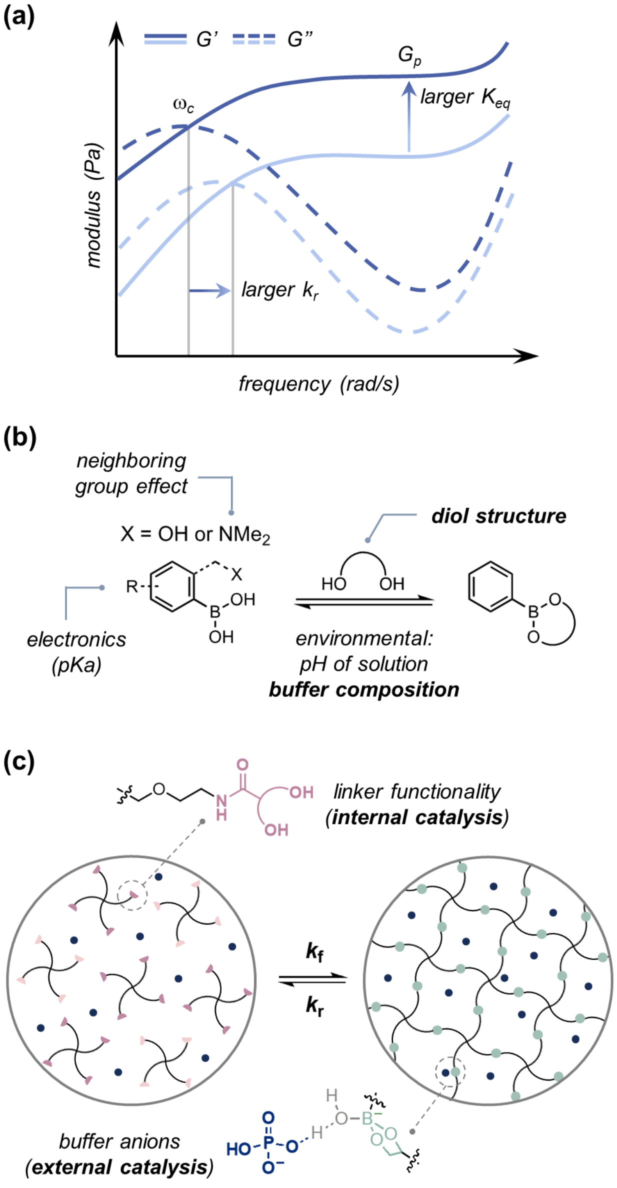

Figure 1. (a) Translation of molecular parameters into macroscopic network properties. Solid lines and dashed lines represent storage modulus (G') and loss modulus (G'') of each material with distinct molecular parameter, respectively. The binding constant (K_{eq}) relates to the stiffness (plateau modulus, G_p) while the rate of dissociation (k_r) determines the viscoelasticity in dissociative networks. (b) Summary of factors affecting the boronic acid–diol reversible condensation and focus of this study (in bold). (c) This work uncovers internal catalysis in boronic ester networks by the linker used for diol conjugation, and external catalysis by buffering anions.

The dynamic reaction between boronic acids and diols occurs via multi-step mechanisms and are sensitive to many factors: pKa of the boronic acid and diol, sterics and dihedral angle of the diol, pH of the solution, and buffer composition and concentration (**Figure 1b**).[10, 28, 29] As a result, the reaction landscape varies significantly depending on the choice of boronic acid, diol partner, and reaction conditions. Efforts to understand how these factors affect the thermodynamics of the dynamic bond have focused on maximizing the binding affinity (K_{eq}) at physiological pH.[10, 28, 30-34] Those studies have introduced new classes of boronic acids with high binding affinities, such as Wulff-type boronic acids and benzoxaboroles, and identified diols and polyols with high hydrolytic stability (e.g. nopoldiol and salicylhydroxamic acid).[35-40] In contrast, design principles to tune the kinetics of the reaction have not been systematically developed (see Supporting Information (SI), **Table S1** for a summary of kinetic studies).[41-49] Furthermore, factors of particular relevance to polymer networks, such as the conjugation chemistry used to attach the dynamic bond to polymers or commonly used buffers for hydrogels, are not typically included in small-molecule model studies.

Here, we report the effect of diol structure and salt additives on both kinetics and thermodynamics of the reversible boronic acid–diol condensation and their impact on the mechanical properties of boronic ester networks. We measured the exchange kinetics and binding affinity between different diols/polyols and phenylboronic acid (**PBA**) by one-dimensional selective exchange spectroscopy (1D EXSY) and ^{1}H NMR. We then synthesized star polymers with analogous diol/polyol and boronic acid end groups and measured the mechanical properties of the resulting gels using shear rheology. Through these measurements, we uncovered two new factors that affect the mechanics of boronic ester networks: the presence of amide groups proximal to the diol, and the composition of the buffer (**Figure 1c**). We showed that amide groups used to conjugate diols to polymers act as internal catalysts via a solvent-insertion mechanism,[50] accelerating both esterification and hydrolysis. Additionally, we observed salt-dependent rate constants correlated to the pKa of the anion's conjugate acid. These changes in molecular thermodynamics and kinetics are translated into gels with a wide range of mechanical properties, with shear moduli ranging from 1.8 kPa to 27 kPa and relaxation times from 0.1 s to 571 s, based only on changes in diol structure or salt additive. Our results inform new design parameters that can be used to tune boronic ester-based dynamic materials and complement existing studies that have focused on the boronic acid partner. Furthermore, these findings emphasize the importance of designing small-molecule model systems that capture essential components of the polymer network when relating molecular parameters to network properties.

To study the effect of diol structure on boronic ester formation and hydrolysis, we selected a representative 1,2-diol, 1,3-diol, triol, and polyol with varying degrees of flexibility and steric encumbrance (**Figure 2a,** “simplified alcohols”). The reaction kinetics of the reversible condensation between **PBA** and each alcohol were studied by using 1D EXSY. EXSY NMR detects magnetization transfer via chemical exchange, allowing quantitative measurement of the rate of dynamic processes occurring slower than the NMR time scale. In 1D EXSY, a peak of interest is selectively excited, and the intensities of the irradiated and exchanged peaks are monitored as a function of mixing time.

The dynamic reaction was studied under pseudo-first order conditions (see SI for details). Under these conditions, the *ortho*-protons of the boronic acid and ester can be selectively irradiated in the 1D EXSY experiment (**Figure 2b**). The decrease in acid concentration following irradiation with respect to mixing time was fit to a first-order reversible rate law to obtain pseudo-first-order rate constants for the forward (esterification, $k_{\mathrm{obs,f}}$) and reverse (hydrolysis, $k_{\mathrm{obs,r}}$) reactions (**Figure 2c**).[51] These measurements were repeated at several temperatures to determine the activation energies for esterification and hydrolysis (**Figure 2d**).

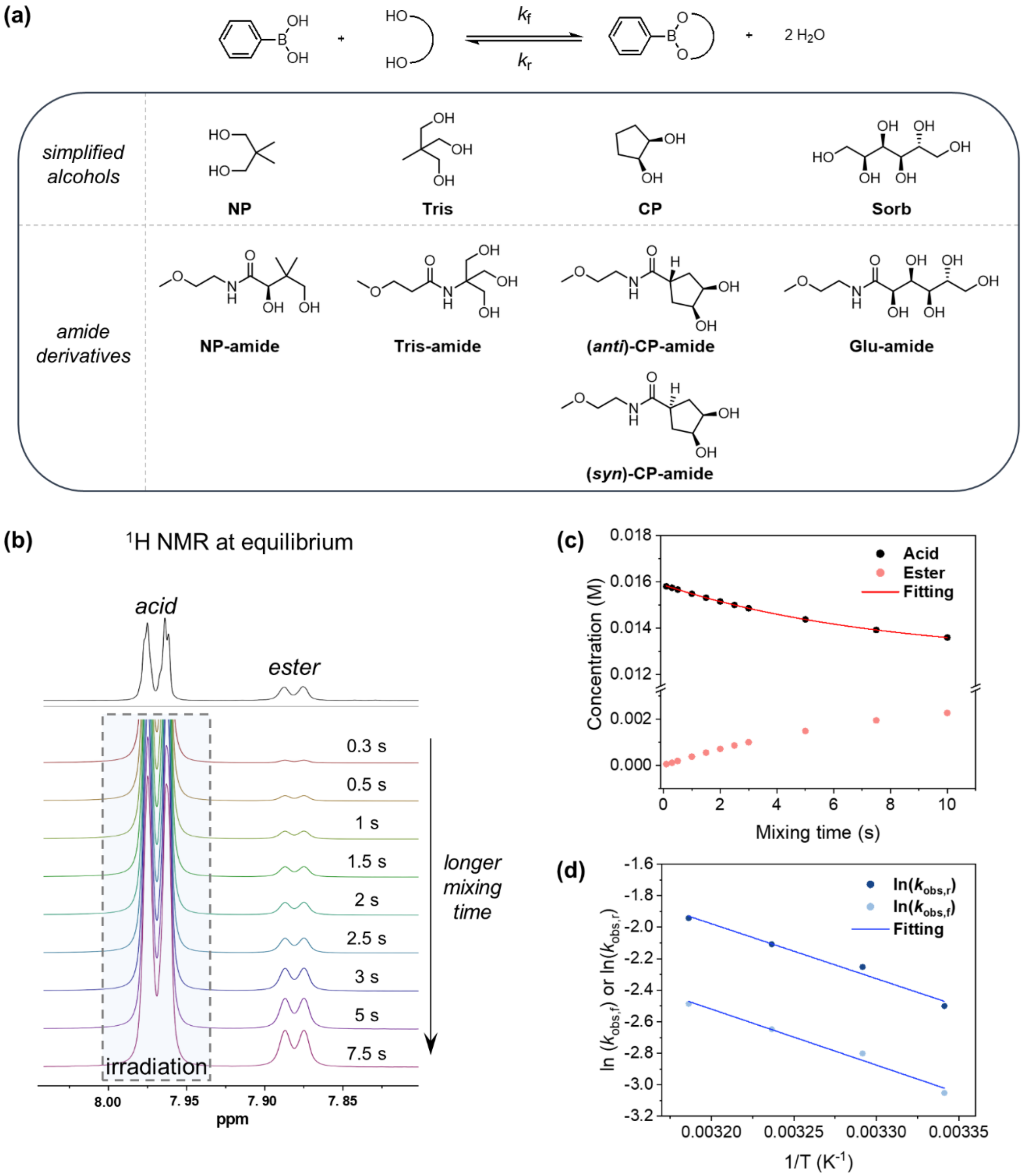

Figure 2. (a) The reversible condensation between **PBA** and alcohols, and the structures of the alcohols used in this study. (b) Representative ^{1}H NMR (top, at equilibrium) and 1D EXSY with different mixing times (bottom) with **PBA** and **NP** at 25 ºC. The peak at 7.97 ppm (*ortho*-proton of **PBA**) is selectively irradiated. (c) Analysis of 1D EXSY data. The concentration change of **PBA** over mixing time was fit with a first-order reversible rate law. (d) Arrhenius plot for pseudo-first-order rate constants at different temperatures; activation energies were calculated from the slope.

The measured kinetic parameters and equilibrium constants for each alcohol are summarized in **Table 1**; activation energies ($E_{a,f}$ for esterification and $E_{a,r}$ for hydrolysis) are reported in **Table S3**. Consistent with previous work,[29] the flexible 1,3-diol neopentylglycol (**NP**) exhibited a significantly lower binding affinity to **PBA** compared to *cis*-1,2-cyclopentanediol (**CP**), which has a locked geometry that favors ester formation but slows kinetics dramatically. Increasing the number of OH groups also enhanced the binding affinity (**NP** < **Tris** < **Sorb**). As the functionality increases, the rate of esterification increases, and the rate of hydrolysis decreases, albeit to a lesser extent.

Table 1. Equilibrium and rate constants for the reversible esterification/hydrolysis of **PBA** with various alcohols.

Alcohols	K_{eq}	$k_{obs,f}$ (s^{-1})	$k_{obs,r}$ (s^{-1})	$k_{rel,f}$[c]	$k_{rel,r}$[c]
NP	0.577 (±0.009)	0.0473 (±0.0004)	0.082 (±0.001)		
Tris	1.389 (±0.006)	0.1100 (±0.0003)	0.0792 (±0.0003)		
Sorb	7.4 (±0.6)	0.23 (±0.01)	0.031 (±0.002)		
CP	15[a] (±2)	0.0216 (±0.0004)	0.0014[b] (±0.0002)		
Tris-amide	0.182 (±0.006)	2.20 (±0.04)	12.1 (±0.3)	20	150
NP-amide	0.877 (±0.005)	0.327 (±0.001)	0.373 (±0.002)	6.9	4.5
(*syn*)-CP-amide	1.45 (±0.02)	0.210 (±0.002)	0.145 (±0.002)	9.7	100
(*anti*)-CP-amide	5.4 (±0.4)	0.107 (±0.006)	0.020 (±0.001)	5.0	14
Glu-amide	6.4 (±0.5)	0.70 (±0.03)	0.110 (±0.008)	3.0	3.5

[a] Estimated using K_{eq} = ([ester][H_2O]^2)/([acid][diol]) because hydrolysis was too slow for the rate constant to be extracted by fitting; see SI for details. [b] Estimated from K_{eq} using $k_{obs,r} = k_{obs,f}/K_{eq}$. [c] Calculated by k_{obs} (amide derivatives)/k_{obs} (simplified alcohols).

We next synthesized star polymers with end groups that contain the structures of the simplified alcohols (**Figure 3a**; see SI for synthetic details). A mixture of *anti* and *syn* diastereomers was used to prepare **PEG-CP**; as a result, its end groups represent a 4:1 ratio of *anti* and *syn* diastereomers in all cases unless otherwise noted (see SI for assignment). Each alcohol-terminated polymer was mixed with **PEG-PBA** in a 1:1 ratio to form a 10 w/v% solution in propylene carbonate containing 1% (v/v) D_2O. This solvent mixture was required based on the low binding constants of some of the alcohols tested, which preclude gelation in fully aqueous environments. The gels were characterized by oscillatory shear rheology within the linear viscoelastic regime to determine the frequency-independent plateau modulus (G_p) (**Figure 3b**; see SI for amplitude sweeps).

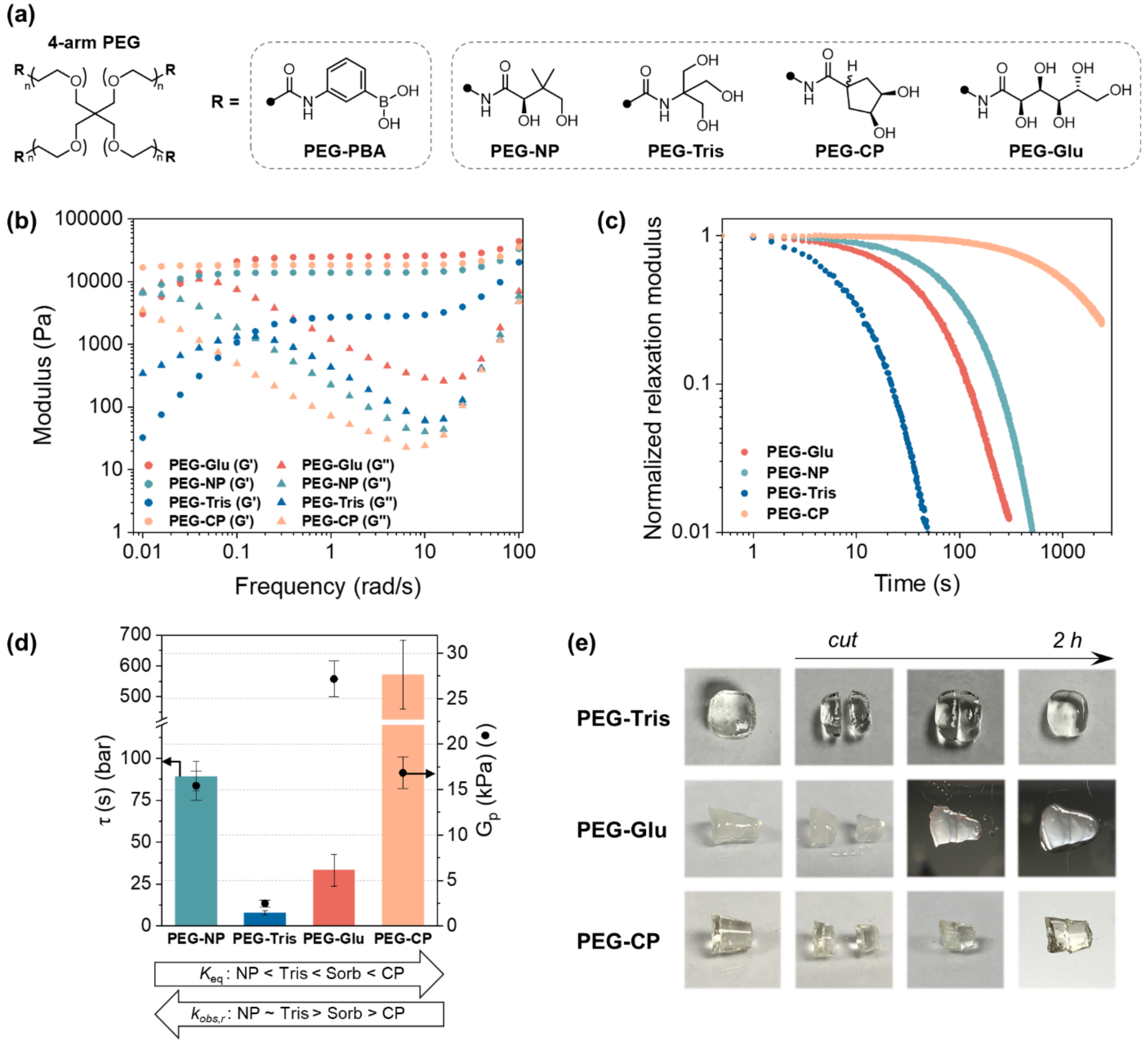

Figure 3. Mechanical and self-healing properties of the gels formed from 4-arm **PEG-PBA** and **PEG-alcohol** (1:1, 10 w/v% in propylene carbonate with 1% D_2O). (a) Chemical structures of modified PEG polymers. **PEG-CP** end groups represent a mixture of diastereomers (4:1 *anti*:*syn*; see SI for assignment). (b) Frequency sweeps at 5% strain obtained by oscillatory shear rheology. (c) Normalized stress relaxation profiles following 5% shear step strain. (d) Calculated τ for the different gels (bar graph, left axis) and their plateau moduli, G_p (black dot, right axis). Mechanical data are the average of 3 samples; error is the standard deviation of the mean. (e) Photographs of **PEG-Tris**, **PEG-Glu** and **PEG-CP** gels undergoing self-healing.

In a dynamic network, the number of elastically active polymer strands, which determines G_p, is dictated by K_{eq} of the crosslink. Tibbitt recently modified the phantom network model to directly relate G_p to K_{eq} in dynamic networks and demonstrated the validity of this model in a boronic ester hydrogel.[21] Based on the K_{eq} values obtained for the simplified alcohol in **Table 1**, we expected the relative plateau moduli of the corresponding gels to follow the trend **PEG-NP** < **PEG-Tris** <

PEG-Glu < **PEG-CP**. However, we observed that the moduli followed the trend **PEG-Tris** << **PEG-NP** < **PEG-CP** < **PEG-Glu** (**Figure 3d**).

To relate the kinetics of the dynamic bond and the viscoelasticity of the gels, we applied a step strain (5%) to the gels and measured the stress relaxation over time (**Figure 3c**). These data were fit to a Maxwell model to obtain the characteristic relaxation time τ, the time required for the material to relax stress to 1/e of its initial value. The theoretical foundation established by Semenov and Rubinstein revealed an inverse relationship between τ and the dissociation rate of the crosslink ($\tau \propto 1/ k_{\mathrm{obs,r}}$),[23, 24] and experimental studies have confirmed this relationship.[17-21, 26, 52-54] Based on the measured $k_{\mathrm{obs,r}}$ values of the simplified alcohols, we expected to observe the trend **PEG-NP** ~ **PEG-Tris** < **PEG-Glu** << **PEG-CP**. However, the trend in relaxation times was **PEG-Tris** < **PEG-Glu** < **PEG-NP** << **PEG-CP** (**Figure 3d**).

Analogously, the rate of self-healing ability in the network should be determined by the rate of crosslink formation ($k_{\mathrm{obs,f}}$).[26, 27, 55] We qualitatively compared self-healing of **PEG-Tris, PEG-Glu** and **PEG-CP** gels by cutting and re-forming the gels, and observed the fastest self-healing in **PEG-Tris** (**Figure 3e**). Based on the measured $k_{\mathrm{obs,f}}$ trend, we expect self-healing to occur fastest for **PEG-Glu.** Taken together, the discrepancies between the small-molecule parameters and the mechanical properties of the networks led us to re-evaluate the use of simplified alcohols as model compounds.

The key structural difference between the simplified alcohols in **Figure 2a** and the crosslinkers in the gel is the presence of amide groups used for conjugation. Previously, our lab has taken advantage of photoswitchable Lewis basic groups proximal to the boronic ester to modulate the kinetics and thermodynamics of its dynamic covalent reactions.[56-58] Anslyn has shown that the basic aminomethyl group in Wulff-type boronic acids catalyzes the addition and elimination of alcohols and water.[42, 59] However, analogous internal catalytic effects for the diol component of this dynamic covalent reaction are far less studied. Hall showed that the proximity of an ether linkage to nopoldiol had a 1.4–1.8-fold effect on esterification rate,[36] but the effect on hydrolysis rate was not quantified. We hypothesized that the amide groups introduced for polymer functionalization perturb the rate and equilibrium constants of the esterification and hydrolysis reactions, through inductive effects, direct coordination to the boron center,[60, 61] or internal catalysis.[62, 63]

Therefore, we synthesized amide derivatives of each alcohol (**Figure 1a,** “amide derivatives”) and measured the kinetics of their dynamic reactions with **PBA** using 1D EXSY (**Table 1**). Indeed, we observed dramatic increases in both esterification and hydrolysis rates for the amide derivatives compared to their simplified alcohol counterparts. These increases ranged from a factor of 3 (**Sorb** vs. **Glu-amide**) to greater than an order of magnitude (**Tris** vs. **Tris-amide**, 20-fold increase in $k_{\mathrm{obs,f}}$ and 150-fold increase in $k_{\mathrm{obs,r}}$). With **Glu-amide**, we observed an additional peak that undergoes exchange with both acid and ester (**Figure S18**). We propose this peak is an intermediate species as multiple binding modes can exist with ring-opened gluconolactone.[18]

To obtain insight into the relative contributions of inductive and neighboring-group effects, we prepared the *anti* and *syn* diastereomers of **CP-amide** and separately measured their reaction kinetics with **PBA**. Relative to unfunctionalized **CP**, the minor isomer of **CP-amide** (*syn*) experiences more significant rate acceleration (9.7-fold for esterification and 100-fold for hydrolysis) than the major isomer (*anti*, 5.0-fold and 14-fold, respectively) (**Table 1**). We propose that **(*syn*)-CP-amide** experiences greater rate acceleration than the *anti* diastereomer because the amide carbonyl is on the same face of the cyclopentane ring as the diol and is thus well positioned to activate incoming nucleophiles (**Figure S19**). Furthermore, using ^{11}B NMR, we obtained evidence that the boronic ester of **NP-amide** forms a solvent-inserted tetrahedral species in methanol-d$_4$, which is not observed with **NP** (**Figure S20**).[50, 64] These results suggest that internal catalysis occurs via a solvent-assisted mechanism, wherein the amide carbonyl facilitates proton transfer when water or alcohol attacks the boron center.

The amide derivatives exhibited more pronounced rate acceleration for hydrolysis than for esterification, except for **NP-amide**. As a result, the binding constants for **Tris-amide**, **CP-amide**, and **Glu-amide** with **PBA** are lower than those of their simplified alcohol counterparts. Therefore, when the amide effect is considered, the trend in binding affinities for the amide model systems (**Tris-amide** < **NP-amide** < **CP-amide** < **Glu-amide**) is consistent with the trend in plateau modulus observed for the gels. Furthermore, the self-healing trends for the networks are qualitatively consistent with the $k_{\mathrm{obs,f}}$ trends for the amide derivatives, with **Tris-amide** and **PEG-Tris** displaying the highest $k_{\mathrm{obs,f}}$ and self-healing rate, respectively.

The $k_{\mathrm{obs,r}}$ values predict a trend in bulk relaxation times (**Tris-amide** < **NP-amide** < **Glu-amide** < **(*anti*)-CP-amide**) that more closely resembles the gel data. The ratio of *anti*:*syn* isomers in **PEG-CP** affects the relaxation time, with a greater fraction of *syn* isomer (*anti*:*syn* = 1.5:1 vs. 4:1) corresponding to faster stress relaxation (τ = 355 vs. 571 s), again providing evidence for the relevance of internal catalysis in the mechanism by which the network relaxes stress (**Figure S38**). While the measured rate constant for **Glu-amide** hydrolysis is ~3-fold slower than **NP-amide** hydrolysis based on our EXSY experiments, **PEG-Glu** relaxes stress ~2-fold faster than **PEG-NP**. However, this discrepancy is ascribed in part to the buildup of an intermediate in the dynamic reaction of **Glu-amide**, which may affect the rate constants measured by EXSY.

Overall, our data agree with the paradigm first articulated by Craig for dynamic networks: "strong means slow", meaning that the gels that resist flow have slower kinetics for the crosslink-breaking step.[53] Previous studies of supramolecular networks have shown that the frequency sweeps for chemically distinct networks can be superimposed when scaled to a molecular parameter such as k_r or $E_{a,r}$ ("time-crosslinker superposition").[17, 65] However, those systems undergo flow through single-step, dissociative mechanisms. For our boronic ester networks, it was not possible to superimpose the frequency sweep data by scaling to $1/k_{obs,r}$ (**Figure S37**). We ascribe these differences to the complexity of boronic ester hydrolysis, a multi-step mechanism in which the dominant pathway and speciation can change depending on the structure of the boronic acid and diol, and environmental factors like solvent and pH.[41, 48, 66] Consistent with changes in mechanism or rate-limiting step, the small-molecule activation energies are not consistently lowered by the presence of an internal catalyst (e.g. $E_{a,r}$ is 20 kJ/mol for **Tris** and 36 kJ/mol for **Tris-amide**; see **Table S3**).

Many boronic ester-based hydrogels are designed for biomedical applications, so are typically formed and studied in the presence of buffers or media containing inorganic salts, amino acids, glucose, and vitamins. While previous studies have focused on the pH of the medium rather than the buffer itself, Springsteen and Wang showed that the binding affinity of a catechol dye to **PBA** is sensitive to buffer composition and concentration.[30, 67] Furthermore, London and Gabel showed that the presence of phosphate anion increased the dissociation rate of 4-fluorophenylboronic esters.[68] In the course of our studies, we also observed significant changes in viscoelasticity of gels based on the identity and concentration of buffer salts. Therefore, we used 1D EXSY to systematically determine the effect of ions on the rate of boronic ester exchange. **NP** was used as the model diol for this study, and various salts were introduced to the solution. To rule out any changes in rate due to pH, the pH of each solution was adjusted to 7 using either DCl or NaOD.

The pseudo-first-order rate constants for esterification and hydrolysis in the presence of various salts are shown in **Table 2**. Using a common buffer, phosphate-buffered saline (PBS), we observed two orders of magnitude increase of the rate constants for both the forward and reverse reactions. The effect of phosphate anion was further confirmed with $NBu_4H_2PO_4$, which revealed similar rate acceleration. London and Gabel proposed that phosphate anions catalyze proton transfer from water during hydrolysis.[68] We further observed that the extent of acceleration was correlated with the pKa of the conjugate acid: KOAc provides ~7-fold acceleration, compared to D_2O alone, and NBu_4PF_6 shows no effect (see **Table S4** for additional salts). K_{eq} was not affected by salt in acetone (**Table 2**), but a two-fold change was observed in propylene carbonate (**Figure S43**).

Table 2. Rate constants for the reversible esterification/hydrolysis of **PBA** with **NP** in the presence of different salts at pH 7.

Salt	pKa[a]	$k_{obs,f}$ (s^{-1})	$k_{obs,r}$ (s^{-1})
No salt	-	0.0473 (±0.0004)	0.082 (±0.001)
PBS (NaH_2PO_4 + Na_2HPO_4)	$H_2PO_4^-$ = 7.21	5.59 (±0.07)	8.2 (±0.1)
$NBu_4H_2PO_4$		4.90 (±0.06)	7.9 (±0.1)
KOAc	CH_3COOH = 4.76	0.371 (±0.002)	0.574 (±0.005)
NBu_4PF_6	-	0.0587 (±0.0006)	0.095 (±0.001)

[a]From pKa data compiled by R. Williams.[69]

We anticipated that the dramatic effects on hydrolysis rate would also translate to the viscoelasticity of boronic ester gels. Indeed, compared to the **PEG-NP** gel without salts, relaxation times are 10 and 1000 times faster in the presence of 0.01 M KOAc and 0.01 M $NBu_4H_2PO_4$, respectively (**Figure 4a**). This 1000-fold range in relaxation times is visually apparent and is achieved solely through the addition of salts, without any change in pH (**Figure 4b**).

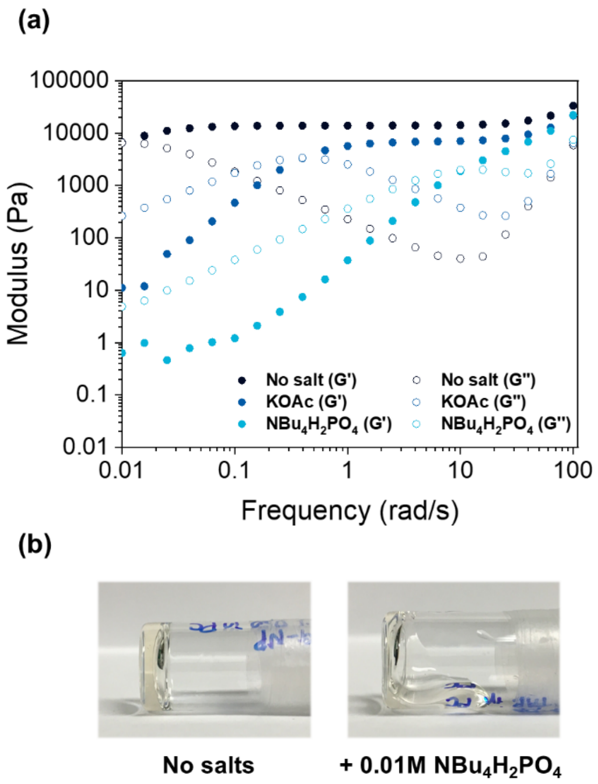

Figure 4. Effects of anion coordination on the mechanical properties of the **PEG-NP** gels (10 w/v% in propylene carbonate with 1% 1M salt in D_2O) formed with solution containing different salts (final concentration of salt: 0.01M). pH of the 1M stock solution of the salt in D_2O was adjusted to 7 with either DCl or NaOD. (a) Frequency sweep with 5% strain. (b) Photographs of **PEG-NP** gels at pH 7 in the absence and the presence of 0.01M $NBu_4H_2PO_4$ salts.

Small-molecule model studies, including our own,[58] are often performed with simple diols like ethylene glycol or fructose in organic solvents such as DMSO, which simplifies analysis. In comparison, the attachment of diols to polymers requires the installation of Lewis basic functional groups like amides, triazoles,[70] and oximes.[71] Furthermore, the resulting materials are often studied in complex aqueous environments like buffer or media. Our findings suggest that small-molecule model studies based on simple diols in organic solvents do not sufficiently capture the behavior of materials, particularly in the translation from molecular kinetics to dynamic mechanical properties.

By comparing the small-molecule kinetics of dynamic covalent reactions to the macroscopic properties of covalent adaptable networks, we have discovered two factors that affect gel mechanics by accelerating boronic acid esterification and hydrolysis: proximal amides commonly used to conjugate crosslinkers to polymers, and anions found in buffers and media. The extent of this rate acceleration can be precisely tuned through the position of the amide relative to the diol and the pKa of the anion's conjugate acid, and therefore can be viewed as tunable design parameters for dynamic materials. The internal catalysis effect may extend to other Lewis basic groups used for polymer modification, with both distance and three-dimensional structure influencing the magnitude of this effect[36, 70, 71], or to other classes of boronic acids such as benzoxaboroles and Wulff-type boronic acids. These effects could be exploited in the design of dynamic materials that change physical properties in response to anions or diols. We envision this work will contribute to a growing understanding of the boronic ester dynamic bond and provide strategies to molecularly engineer dynamic materials.

Supporting Information

Synthetic procedures, EXSY NMR spectra and fitting, rheology data, ^{11}B, ^{1}H, and ^{13}C NMR spectra.

Acknowledgements

The small-molecule studies in this work were supported by the National Science Foundation under CAREER award CHE-1847948, and the network studies were supported by the National Institute of General Medical Sciences of the National Institutes of Health under award number R01GM132677. This content is solely the responsibility of the authors and does not necessarily represent the official views of the National Science Foundation or National Institutes of Health. J.A.K. is supported by a Sloan Research Fellowship and a Dreyfus Teacher-Scholar Award. This work made use of NMR and MS instrumentation at the Integrated Molecular Structure Education and Research Center (IMSERC) at Northwestern, which has received support from the NSF (NSF CHE-9871268); Soft and Hybrid Nanotechnology Experimental (SHyNE) Resource (NSF ECCS-1542205); the State of Illinois and International Institute for Nanotechnology. Rheological measurements were performed at the MatCI Facility, which receives support from the MRSEC Program (NSF DMR-1720139) of the Materials Research Center at Northwestern University.

References

1. Wu, X.; Li, Z.; Chen, X. X.; Fossey, J. S.; James, T. D.; Jiang, Y. B., Selective sensing of saccharides using simple boronic acids and their aggregates. *Chem. Soc. Rev.* **2013,** *42* (20), 8032-48.
2. Bian, Z.; Liu, A.; Li, Y.; Fang, G.; Yao, Q.; Zhang, G.; Wu, Z., Boronic acid sensors with double recognition sites: a review. *Analyst* **2020,** *145* (3), 719-744.
3. Brooks, W. L.; Sumerlin, B. S., Synthesis and Applications of Boronic Acid-Containing Polymers: From Materials to Medicine. *Chem. Rev.* **2016,** *116* (3), 1375-97.
4. Cambre, J. N.; Sumerlin, B. S., Biomedical applications of boronic acid polymers. *Polymer* **2011,** *52* (21), 4631-4643.
5. Galbraith, E.; James, T. D., Boron based anion receptors as sensors. *Chem. Soc. Rev.* **2010,** *39* (10), 3831-42.

6. Guan, Y.; Zhang, Y., Boronic acid-containing hydrogels: synthesis and their applications. *Chem. Soc. Rev.* **2013,** *42* (20), 8106-21.
7. Stubelius, A.; Lee, S.; Almutairi, A., The Chemistry of Boronic Acids in Nanomaterials for Drug Delivery. *Acc. Chem. Res.* **2019,** *52* (11), 3108-3119.
8. Ryu, J. H.; Lee, G. J.; Shih, Y. V.; Kim, T. I.; Varghese, S., Phenylboronic Acid-polymers for Biomedical Applications. *Curr. Med. Chem.* **2019,** *26* (37), 6797-6816.
9. Marco-Dufort, B.; Willi, J.; Vielba-Gomez, F.; Gatti, F.; Tibbitt, M. W., Environment Controls Biomolecule Release from Dynamic Covalent Hydrogels. *Biomacromolecules* **2021,** *22* (1), 146-157.
10. Marco-Dufort, B.; Tibbitt, M. W., Design of moldable hydrogels for biomedical applications using dynamic covalent boronic esters. *Mater. Today Chem.* **2019**, *12*, 16-33.
11. Zhang, W.; Jin, Y., *Dynamic Covalent Chemistry: Principles, Reactions, and Applications*; Wiley-VCH, Print. 2017.
12. Jin, Y.; Yu, C.; Denman, R. J.; Zhang, W., Recent advances in dynamic covalent chemistry. *Chem. Soc. Rev.* **2013,** *42* (16), 6634-54.
13. Rowan, S. J.; Cantrill, S. J.; Cousins, G. R. L.; Sanders, J. K. M.; Stoddart, J. F., Dynamic Covalent Chemistry. *Angew. Chem. Int. Ed.* **2002,** *41* (6), 898-952.
14. Tang, S.; Richardson, B. M.; Anseth, K. S., Dynamic covalent hydrogels as biomaterials to mimic the viscoelasticity of soft tissues. *Prog. Mater. Sci.* **2021,** *120*, 100738.
15. Robinson, L. L.; Self, J. L.; Fusi, A. D.; Bates, M. W.; Read de Alaniz, J.; Hawker, C. J.; Bates, C. M.; Sample, C. S., Chemical and Mechanical Tunability of 3D-Printed Dynamic Covalent Networks Based on Boronate Esters. *ACS Macro Lett.* **2021,** *10* (7), 857-863.
16. Kloxin, C. J.; Bowman, C. N., Covalent adaptable networks: smart, reconfigurable and responsive network systems. *Chem. Soc. Rev.* **2013,** *42* (17), 7161-73.
17. Yount, W. C.; Loveless, D. M.; Craig, S. L., Small-molecule dynamics and mechanisms underlying the macroscopic mechanical properties of coordinatively cross-linked polymer networks. *J. Am. Chem. Soc.* **2005,** *127* (41), 14488-96.
18. Figueiredo, T.; Cosenza, V.; Ogawa, Y.; Jeacomine, I.; Vallet, A.; Ortega, S.; Michel, R.; Olsson, J. D. M.; Gerfaud, T.; Boiteau, J. G.; Jing, J.; Harris, C.; Auzely-Velty, R., Boronic acid and diol-containing polymers: how to choose the correct couple to form "strong" hydrogels at physiological pH. *Soft Matter* **2020,** *16* (15), 3628-3641.
19. Tang, S.; Olsen, B. D., Relaxation Processes in Supramolecular Metallogels Based on Histidine–Nickel Coordination Bonds. *Macromolecules* **2016,** *49* (23), 9163-9175.
20. Tan, C. S. Y.; Agmon, G.; Liu, J.; Hoogland, D.; Janeček, E.-R.; Appel, E. A.; Scherman, O. A., Distinguishing relaxation dynamics in transiently crosslinked polymeric networks. *Polym. Chem.* **2017,** *8* (35), 5336-5343.
21. Marco-Dufort, B.; Iten, R.; Tibbitt, M. W., Linking Molecular Behavior to Macroscopic Properties in Ideal Dynamic Covalent Networks. *J. Am. Chem. Soc.* **2020,** *142* (36), 15371-15385.
22. Parada, G. A.; Zhao, X., Ideal reversible polymer networks. *Soft Matter* **2018,** *14* (25), 5186-5196.
23. Semenov, A. N.; Rubinstein, M., Thermoreversible Gelation in Solutions of Associative Polymers. 1. Statics. *Macromolecules* **1998,** *31* (4), 1373-1385.
24. Rubinstein, M.; Semenov, A. N., Thermoreversible Gelation in Solutions of Associating Polymers. 2. Linear Dynamics. *Macromolecules* **1998,** *31* (4), 1386-1397.
25. Van Herck, N.; Maes, D.; Unal, K.; Guerre, M.; Winne, J. M.; Du Prez, F. E., Covalent Adaptable Networks with Tunable Exchange Rates Based on Reversible Thiol-yne Cross-Linking. *Angew. Chem. Int. Ed.* **2020,** *59* (9), 3609-3617.
26. Cromwell, O. R.; Chung, J.; Guan, Z., Malleable and Self-Healing Covalent Polymer Networks through Tunable Dynamic Boronic Ester Bonds. *J. Am. Chem. Soc.* **2015,** *137* (20), 6492-5.
27. FitzSimons, T. M.; Oentoro, F.; Shanbhag, T. V.; Anslyn, E. V.; Rosales, A. M., Preferential Control of Forward Reaction Kinetics in Hydrogels Crosslinked with Reversible Conjugate Additions. *Macromolecules* **2020,** *53* (10), 3738-3746.

28. Yan, J.; Springsteen, G.; Deeter, S.; Wang, B., The relationship among pKa, pH, and binding constants in the interactions between boronic acids and diols—it is not as simple as it appears. *Tetrahedron* **2004,** *60* (49), 11205-11209.
29. Roy, C. D.; Brown, H. C., Stability of boronic esters – Structural effects on the relative rates of transesterification of 2-(phenyl)-1,3,2-dioxaborolane. *J. Organomet. Chem.* **2007,** *692* (4), 784-790.
30. Bosch, L. I.; Fyles, T. M.; James, T. D., Binary and ternary phenylboronic acid complexes with saccharides and Lewis bases. *Tetrahedron* **2004,** *60* (49), 11175-11190.
31. Peters, J. A., Interactions between boric acid derivatives and saccharides in aqueous media: Structures and stabilities of resulting esters. *Coord. Chem. Rev.* **2014,** *268*, 1-22.
32. Brooks, W. L. A.; Deng, C. C.; Sumerlin, B. S., Structure-Reactivity Relationships in Boronic Acid-Diol Complexation. *ACS Omega* **2018,** *3* (12), 17863-17870.
33. Cheng, Y.; Ni, N.; Yang, W.; Wang, B., A new class of fluorescent boronic acids that have extraordinarily high affinities for diols in aqueous solution at physiological pH. *Chem. Eur. J.* **2010,** *16* (45), 13528-38.
34. Martínez-Aguirre, M. A.; Flores-Alamo, M.; Yatsimirsky, A. K., Thermodynamic and structural study of complexation of phenylboronic acid with salicylhydroxamic acid and related ligands. *Appl. Organomet. Chem.* **2018,** *32* (8).
35. Deng, C. C.; Brooks, W. L. A.; Abboud, K. A.; Sumerlin, B. S., Boronic Acid-Based Hydrogels Undergo Self-Healing at Neutral and Acidic pH. *ACS Macro Lett.* **2015,** *4* (2), 220-224.
36. Akgun, B.; Hall, D. G., Fast and Tight Boronate Formation for Click Bioorthogonal Conjugation. *Angew. Chem. Int. Ed.* **2016,** *55* (12), 3909-13.
37. Roberts, M. C.; Hanson, M. C.; Massey, A. P.; Karren, E. A.; Kiser, P. F., Dynamically Restructuring Hydrogel Networks Formed with Reversible Covalent Crosslinks. *Adv. Mater.* **2007,** *19* (18), 2503-2507.
38. Wulff, G., Selective binding to polymers via covalent bonds. The construction of chiral cavities as specific receptor sites. *Pure Appl. Chem.* **1982,** *54* (11), 2093-2102.
39. Stolowitz, M. L.; Ahlem, C.; Hughes, K. A.; Kaiser, R. J.; Kesicki, E. A.; Li, G.; Lund, K. P.; Torkelson, S. M.; Wiley, J. P., Phenylboronic acid-salicylhydroxamic acid bioconjugates. 1. A novel boronic acid complex for protein immobilization. *Bioconjug. Chem.* **2001,** *12* (2), 229-39.
40. Dowlut, M.; Hall, D. G., An improved class of sugar-binding boronic acids, soluble and capable of complexing glycosides in neutral water. *J. Am. Chem. Soc.* **2006,** *128* (13), 4226-7.
41. Furikado, Y.; Nagahata, T.; Okamoto, T.; Sugaya, T.; Iwatsuki, S.; Inamo, M.; Takagi, H. D.; Odani, A.; Ishihara, K., Universal reaction mechanism of boronic acids with diols in aqueous solution: kinetics and the basic concept of a conditional formation constant. *Chem. Eur. J.* **2014,** *20* (41), 13194-202.
42. Collins, B. E.; Metola, P.; Anslyn, E. V., On the Rate of Boronate Ester Formation in ortho-Aminomethyl Functionalized Phenyl Boronic Acids. *Supramol. Chem.* **2013,** *25* (2), 79-86.
43. Tomsho, J. W.; Benkovic, S. J., Elucidation of the mechanism of the reaction between phenylboronic acid and a model diol, Alizarin Red S. *J. Org. Chem.* **2012,** *77* (5), 2098-106.
44. Pizer, R.; Tihal, C., Equilibria and Reaction Mechanism of the Complexation of Methylboronic Acid with Polyols. *Inorg. Chem.* **1992,** (31), 3243-3247.
45. Monajemi, H.; Cheah, M. H.; Lee, V. S.; Zain, S. M.; Tajuddin Wan Abdullah, W. A., On the kinetics and reaction mechanisms of boronic acid in interaction with diols for non-enzymatic glucose monitoring applications: a hybrid DFT study. *RSC Adv.* **2014,** *4* (21), 10505-10513.
46. Pizer, R. D.; Tihal, C. A., Mechanism of boron acid/polyol complex formation. Commnets on the Trigonal/tetrahedral interconversion on boron. *Polyhedron* **1996,** *15* (19), 3411-3416.
47. Ni, N.; Laughlin, S.; Wang, Y.; Feng, Y.; Zheng, Y.; Wang, B., Probing the general time scale question of boronic acid binding with sugars in aqueous solution at physiological pH. *Bioorg. Med. Chem.* **2012,** *20* (9), 2957-61.

48. Suzuki, Y.; Kusuyama, D.; Sugaya, T.; Iwatsuki, S.; Inamo, M.; Takagi, H. D.; Ishihara, K., Reactivity of Boronic Acids toward Catechols in Aqueous Solution. *J. Org. Chem.* **2020,** *85* (8), 5255-5264.
49. Pizer, R.; Babcock, L., Mechanism of the complexation of boron acids with catechol and substituted catechols. *Inorg. Chem.* **1977,** *16* (7), 1677-1681.
50. Zhu, L.; Shabbir, S. H.; Gray, M.; Lynch, V. M.; Sorey, S.; Anslyn, E. V., A structural investigation of the N-B interaction in an o-(N,N-dialkylaminomethyl)arylboronate system. *J. Am. Chem. Soc.* **2006,** *128* (4), 1222-32.
51. Swartjes, A.; White, P. B.; Lammertink, M.; Elemans, J.; Nolte, R. J. M., Host-Guest Exchange of Viologen Guests in Porphyrin Cage Compounds as Studied by Selective Exchange Spectroscopy (1D EXSY) NMR. *Angew. Chem. Int. Ed.* **2021,** *60* (3), 1254-1262.
52. Sheridan, R. J.; Bowman, C. N., A Simple Relationship Relating Linear Viscoelastic Properties and Chemical Structure in a Model Diels–Alder Polymer Network. *Macromolecules* **2012,** *45* (18), 7634-7641.
53. Yount, W. C.; Loveless, D. M.; Craig, S. L., Strong means slow: dynamic contributions to the bulk mechanical properties of supramolecular networks. *Angew. Chem. Int. Ed.* **2005,** *44* (18), 2746-8.
54. Kuang, X.; Liu, G.; Dong, X.; Wang, D., Correlation between stress relaxation dynamics and thermochemistry for covalent adaptive networks polymers. *Mater. Chem. Front.* **2017,** *1* (1), 111-118.
55. McKinnon, D. D.; Domaille, D. W.; Cha, J. N.; Anseth, K. S., Bis-Aliphatic Hydrazone-Linked Hydrogels Form Most Rapidly at Physiological pH: Identifying the Origin of Hydrogel Properties with Small Molecule Kinetic Studies. *Chem. Mater.* **2014,** *26* (7), 2382-2387.
56. Barsoum, D.; Kalow, J., Remote-controlled exchange rates by photoswitchable internal catalysis of dynamic covalent bonds. *ChemRxiv.* **2021**, DOI: 10.33774/chemrxiv-2021-lwk72.
57. Accardo, J. V.; Kalow, J. A., Reversibly tuning hydrogel stiffness through photocontrolled dynamic covalent crosslinks. *Chem. Sci.* **2018,** *9* (27), 5987-5993.
58. Accardo, J. V.; McClure, E. R.; Mosquera, M. A.; Kalow, J. A., Using Visible Light to Tune Boronic Acid-Ester Equilibria. *J. Am. Chem. Soc.* **2020,** *142* (47), 19969-19979.
59. Sun, X.; Chapin, B. M.; Metola, P.; Collins, B.; Wang, B.; James, T. D.; Anslyn, E. V., The mechanisms of boronate ester formation and fluorescent turn-on in ortho-aminomethylphenylboronic acids. *Nat. Chem.* **2019,** *11* (9), 768-778.
60. Yoshino, J.; Kano, N.; Kawashima, T., Synthesis of organoboron compounds bearing an azo group and substituent effects on their structures and photoisomerization. *Tetrahedron* **2008,** *64* (33), 7774-7781.
61. Kano, N.; Yoshino, J.; Kawashima, T., Photoswitching of the Lewis acidity of a catecholborane bearing an azo group based on the change in coordination number of boron. *Org. Lett.* **2005,** *7* (18), 3909-11.
62. Chen, H.; Ye, H.; Hai, Y.; Zhang, L.; You, L., n --> pi* interactions as a versatile tool for controlling dynamic imine chemistry in both organic and aqueous media. *Chem. Sci.* **2020,** *11* (10), 2707-2715.
63. Delahaye, M.; Winne, J. M.; Du Prez, F. E., Internal Catalysis in Covalent Adaptable Networks: Phthalate Monoester Transesterification As a Versatile Dynamic Cross-Linking Chemistry. *J. Am. Chem. Soc.* **2019,** *141* (38), 15277-15287.
64. Collins, B. E.; Sorey, S.; Hargrove, A. E.; Shabbir, S. H.; Lynch, V. M.; Anslyn, E. V., Probing intramolecular B-N interactions in ortho-aminomethyl arylboronic acids. *J. Org. Chem.* **2009,** *74* (11), 4055-60.
65. Appel, E. A.; Forster, R. A.; Koutsioubas, A.; Toprakcioglu, C.; Scherman, O. A., Activation energies control the macroscopic properties of physically cross-linked materials. *Angew. Chem. Int. Ed.* **2014,** *53* (38), 10038-43.
66. Wulff, G.; Lauer, M.; Böhnke, H., Rapid Proton Transfer as Cause of an Unusually Large Neighboring Group Effect. *Angew. Chem. Int. Ed.* **1984,** *23* (9), 741-742.
67. Springsteen, G.; Wang, B., A detailed examination of boronic acid–diol complexation. *Tetrahedron* **2002,** *58* (26), 5291-5300.

68. London, R. E.; Gabel, S. A., Fluorine-19 NMR Studies of Fluorobenzeneboronic Acids. 1. Interaction Kinetics with Biologically Significant Ligands. *J. Am. Chem. Soc.* **1994,** *116*, 2562-2569.
69. American Chemical Society, Division of Organic Chemistry, *pKa Values in Water Compilation (by R. Williams).* https://organicchemistrydata.org/hansreich/resources/pka/pka_data/pka-compilation-williams.pdf.
70. Lin, M.; Sun, P.; Chen, G.; Jiang, M., The glyco-stereoisomerism effect on hydrogelation of polymers interacting via dynamic covalent bonds. *Chem. Commun.* **2014,** *50* (68), 9779-82.
71. Tarus, D.; Hachet, E.; Messager, L.; Catargi, B.; Ravaine, V.; Auzely-Velty, R., Readily prepared dynamic hydrogels by combining phenyl boronic acid- and maltose-modified anionic polysaccharides at neutral pH. *Macromol. Rapid. Commun.* **2014,** *35* (24), 2089-95.

Table of contents graphic